Interactions of Amyloid β-Protein with Various Gangliosides in Raft-Like Membranes: Importance of GM1 Ganglioside-Bound Form as an Endogenous Seed for Alzheimer Amyloid†

Atsuko Kakio,‡ Sei-ichi Nishimoto,‡ Katsuhiko Yanagisawa,§ Yasunori Kozutsumi,||,⊥ and Katsumi Matsuzaki*,||

Department of Energy and Hydrocarbon Chemistry, Graduate School of Engineering, Kyoto University, Sakyo-ku, Kyoto 606-8501, Japan, Department of Dementia Research, National Institute of Longevity Sciences, Gengo 36-3, Morioka, Obu, 474-8522, Japan, Graduate School of Biostudies, Kyoto University, Sakyo-ku, Kyoto 606-8501, Japan, and Glyco-Chain Expression Laboratory, Supra-Biomolecular System Research, RIKEN Frontier Research System, Wako 351-0198, Japan

Received January 24, 2002; Revised Manuscript Received March 19, 2002

ABSTRACT: GM1 ganglioside-bound amyloid β-protein (GM1-Aβ), found in brains exhibiting early pathological changes of Alzheimer's disease (AD) plaques, has been suggested to accelerate amyloid fibril formation by acting as a seed. We have previously found using dye-labeled Aβ that Aβ recognizes a GM1 cluster, the formation of which is facilitated by cholesterol [Kakio, A., Nishimoto, S., Yanagisawa, K., Kozutsumi, Y., and Matsuzaki, K. (2001) *J. Biol. Chem. 276,* 24985−24990]. In this study, we investigated the ganglioside species-specificity in its potency to induce a conformational change of Aβ, by which ganglioside-bound Aβ acts as a seed for Aβ fibrillogenesis, using a major ganglioside occurring in brains (GM1, GD1a, GD1b, and GT1b) in raft-like membranes composed of cholesterol and sphingomyelin. Aβ recognized ganglioside clusters, the density of which increased with the number of sialic acid residues. Interestingly, however, mixing of gangliosides inhibited cluster formation. In contrast, the affinities of the protein for the clusters were similar irrespective of lipid composition and of the order of 10^6 M^{-1} at 37 °C. Aβ underwent a conformational transition from an α-helix-rich structure to a β-sheet-rich structure with the increase in protein density on the membrane. Ganglioside-bound Aβ proteins exhibited seeding abilities for amyloid formation. GM1-Aβ exhibited the strongest seeding potential, especially under β-sheet-forming conditions. This study suggested that lipid composition including gangliosides and cholesterol strictly controls amyloid formation.

The conversion of soluble, nontoxic amyloid β-protein (Aβ)[1] to aggregated, toxic Aβ rich in β-sheet structures by seeded polymerization is considered to be the key step in the development of Alzheimer's disease (AD) (*1*−*3*). Accumulating evidence suggests that Aβ-GM1 ganglioside interactions are involved in this process: (i) GM1-bound Aβ (GM1-Aβ) was discovered in brains of patients with AD as well as Down's syndrome[2] (*4, 5*). (ii) GM1-Aβ, which has a conformation distinct from that of soluble Aβ (*6*−*11*), has been shown to accelerate the rate of amyloid fibril formation of soluble Aβ in vitro[2] (*9, 12*).

Recently, our group reported that the formation of GM1-Aβ is highly sensitive to lipid environments; GM1-Aβ is more readily formed in a sphingomyelin (SM)/cholesterol matrix mimicking lipid rafts (*13*) than in a phosphatidylcholine (PC) environment (*10*). Furthermore, Aβ recognizes not an individual GM1 molecule but a GM1cluster, the formation of which is facilitated by cholesterol (*11*). Gangliosides other than GM1 have also been found to show affinity for Aβ (*7, 9, 10, 12, 14, 15*). However, the affinity and the number of binding site in raft-like lipid environments have not been determined. Furthermore, ganglioside species-dependent or Aβ secondary structure-dependent facilitation of fibrillogenesis of Aβ has never been studied to date. In this study, acceleration of fibrillogenesis of Aβ via binding to major gangliosides in the brain was systematically investigated and compared with each other. We found that (i) the number of binding sites is roughly proportional to the number of sialic acid residues, (ii) mixing gangliosides inhibits Aβ binding, and (iii) Aβ fibril formation was most

† Supported by Grant-in-Aids for Scientific Research on Priority Areas (C)-Advanced Brain Science Project and (B)-12140202 from Ministry of Education, Science, Sports and Culture, Japan and the Research Grant for Longevity Sciences (11-C01) from the Ministry of Health and Welfare.

* To whom correspondence should be addressed: Telephone: 81 75 753 4574. Fax: 81 75 761 2698. E-mail: katsumim@pharm.kyoto-u.ac.jp.

‡ Graduate School of Engineering, Kyoto University.

§ National Institute of Longevity Sciences.

|| Graduate School of Biostudies, Kyoto University.

⊥ RIKEN Frontier Research System.

[1] Abbreviations: Aβ, amyloid β-protein; AD, Alzheimer's disease; BODYPY-GM1, BODIPYFL C_5-GM1; CD, circular dichroism; DAC, 7-diethylaminocoumarin-3-carbonyl; fAβ, fibrillar Aβ; GM1, monosialoganglioside GM1; GD1a, disialoganglioside GD1a; GD1b, disialoganglioside GD1b; GT1b, trisialoganglioside GT1b; LUV, large unilamellar vesicle; PC, phosphatidylcholine; SM, sphingomyelin; ThT, thioflavin T.

[2] Hayashi, H., Yamaguchi, H., Hasegawa, K., Matsuzaki, K., Lemere, C. A., Selkoe, D. J., Naiki, H., and Yanagisawa, K., manuscript in preparation.

10.1021/bi0255874 CCC: $22.00
Published on Web 05/17/2002

accelerated in the presence of GM1 under β-sheet forming conditions among the gangliosides investigated.

MATERIALS AND METHODS

Peptide. Human Aβ-(1−40) labeled with the 7-diethylaminocoumarin-3-carbonyl group at its N-terminus (DAC-Aβ) was custom synthesized and characterized by Peptide Institute (Minou, Japan) (*11*). The dye-labeled peptide was always handled in light-protected, capped tubes under a nitrogen atmosphere to avoid photodegradation. Unlabeled human Aβ-(1−40) was also purchased from Peptide Institute. The peptides were dissolved in 0.02% ammonia on ice. We removed any aggregates by ultracentrifugation in 500 μL polyallomer tubes at 100000*g*, 4 °C for 3 h (*16*). The supernatant was then mixed with an equal volume of double concentrated buffer (20 mM Tris/300 mM NaCl/4 mM $CaCl_2$, pH 7.4). The aggregational state of the peptide was checked by circular dichroism (CD), thioflavin T assay, and SDS−PAGE (*11*). The peptide concentration of the supernatant was determined in triplicate by Micro BCA protein assay (Pierce, Rockford, IL).

Lipids. Bovine brain gangliosides (GM1, GD1a, GD1b, and GT1b) and cholesterol were purchased from Sigma (St. Louis, MO). GM1 from Avanti (Alabaster, AL) was also used. Bovine brain SM was obtained from Matreya (Pleasant Gap, PA).

Lipid Vesicle Preparation. Large unilamellar vesicles (LUVs) for fluorescence experiments were prepared and characterized as described previously (*17*). Briefly, lipids were mixed in a chloroform−methanol 2:1 (v/v) mixture. The solvent was removed by evaporation in a rotary evaporator. The residual lipid film, after drying under vacuum overnight, was hydrated with buffer (10 mM Tris/150 mM NaCl/2 mM $CaCl_2$, pH 7.4) and vortex-mixed to produce multilamellar vesicles. The suspension was subjected to five cycles of freezing and thawing, and then extruded through polycarbonate filters (100 nm pore size filter, 31 times) using a Liposofast extruder (Avestin, Ottawa, Canada). The lipid concentration was determined in triplicate by phosphorus analysis (*18*).

Small unilamellar vesicles for CD experiments were prepared by sonication of multilamellar vesicles (2 mM $CaCl_2$ in buffer was replaced by 1 mM EDTA) under a nitrogen atmosphere for 15 min (5 min, 3 times) using a probe-type sonicator. Metal debris from the titanium tip of the probe was removed by centrifugation.

Fluorescence. Fluorescence measurements were carried out on a Shimadzu RF-5000 or RF-5300 spectrofluorometer with a cuvette holder thermostated at 37 °C. After blank subtraction (and volume correction in titration experiments), the spectra were corrected using the spectrum correction attachment provided by the manufacturer.

Fluorescence Titration. DAC-Aβ solution (0.5 μM, 2 mL) was titrated with aliquots of a concentrated LUV suspension in a quartz cuvette with gentle stirring. Fluorescence emission spectra were recorded at an excitation wavelength of 430 nm. The titration interval was 3 min, which was confirmed to be sufficient for establishment of binding equilibrium.

Excimer Fluorescence. LUVs containing 5 mol % BODIPY-GM1 (Molecular Probes, Eugene, OR) were placed in a quartz cuvette. Fluorescence emission spectra were recorded at an excitation wavelength of 480 nm. Fluorescence anisotropy, *r*, was determined at an emission wavelength of 520 nm (monomer peak) using polarizers placed in both the excitation and emission light paths (*19*).

$$r = (I_{0-0} - GI_{0-90})/(I_{0-0} + 2GI_{0-90}) \quad (1)$$

$$G = I_{90-0}/I_{90-90} \quad (2)$$

Fluorescence intensity was denoted by *I*, and the suffixes indicate polarization (in degrees) of the excitation−emission beams. Fluorescence intensity of the corresponding blank sample without BODIPY-GM1 was negligible.

CD. Native human Aβ-(1−40) (15 μM) in buffer (10 mM Tris/150 mM NaCl/1 mM EDTA, pH 7.4) was used for CD measurements. CD spectra were measured on a Jasco J-720 apparatus interfaced to an NEC PC9801 microcomputer, using a 1-mm path-length quartz cell to minimize the absorbance due to buffer components. The instrumental outputs were calibrated with nonhygroscopic ammonium *d*-camphor-10-sulfonate (*20*). Eight scans were averaged for each sample. The averaged blank spectra (vesicle suspension or buffer) were subtracted.

Seeding Assay. Native human Aβ-(1−40) (final concentration, 15 μM) in buffer (10 mM Tris/150 mM NaCl/1 mM EDTA, pH 7.4) was incubated with SUVs composed of ganglioside/cholesterol/SM (20/40/40) at various ganglioside/Aβ ratios for 1 day at 37 °C. SUVs were used for direct comparison with CD studies. As a positive control, Aβ-(1−40) (final concentration, 15 μM) was incubated with a small amount (0.75 μM) of fibrillar Aβ (fAβ) as a seed that was prepared by a long incubation of un-ultracentrifuged 100 μM Aβ-(1−40) solution at 37 °C followed by 15 min sonication. Amyloid formation was estimated by thioflovin-T (ThT) assay (*21*, *22*). ThT was obtained from Aldrich (Milwaukee, WI). The sample (final Aβ concentration 0.5 μM) was added to 5 μM ThT solution in 50 mM glycine buffer (pH 8.5). Fluorescence at 490 nm was measured at an excitation wavelength of 446 nm. A calcein solution (1 μM) in 10 mM Tris/150 mM NaCl/1 mM EDTA (pH 7.4) buffer was used as a fluorescence standard.

RESULTS

Aβ Binding. Binding of DAC-Aβ to LUVs of various lipid compositions was estimated on the basis of DAC fluorescence. The dye-labeled peptide behaves very similarly to the native peptide and therefore faithfully reports Aβ-ganglioside interactions (*11*). The DAC fluorophore is practically nonfluorescent in aqueous environments, whereas membrane binding results in a large increase in fluorescence intensity accompanied by a blue shift in the emission maximum from 483 to 470 nm (*11*). As a quantitative measure, relative fluorescence enhancement, *R*, is defined as follows:

$$R = (F - F_0)/F_0 \quad (3)$$

Fluorescence intensities at 470 nm in the presence and absence of LUVs are denoted by F and F_0, respectively. Figure 1A shows the importance of the lipid environment surrounding GM1 for DAC-Aβ binding. The R value is plotted as a function of lipid-to-peptide ratio. DAC-Aβ bound to micellar GM1 (closed circles) as well as GM1 in a raft-

Table 1: Parameters for Binding of DAC-Aβ to Ganglioside-containing Membranes at 37 °C

lipid composition	R_{max}	K (10^6 M^{-1})[a]	α[a]	x_{max}[a]
GM1 micelle	9.2 ± 0.2	9.5 ± 1.5	0	0.099 ± 0.005
GM1/cholesterol/SM (20/40/40)	11.4 ± 0.5	6.6 ± 1.3	0	0.016 ± 0.002
GD1a/cholesterol/SM (20/40/40)	9.9 ± 0.3	4.4 ± 1.8	1.8	0.045 ± 0.005
GD1b/cholesterol/SM (20/40/40)	10.1 ± 0.4	5.3 ± 0.8	0	0.039 ± 0.004
GT1b/cholesterol/SM (20/40/40)	9.2 ± 0.2	7.5 ± 1.4	0	0.060 ± 0.005
GT1b/cholesterol/SM (10/45/45)	9.4 ± 0.3	8.6 ± 0.9	0	0.008 ± 0.001
GM1/GD1a/GD1b/GT1b/cholesterol/SM (5/5/5/5/40/40)	8.3 ± 0.0	4.9 ± 0.2	0	0.011 ± 0.000

[a] Binding parameters from eqs 4 and 5 are the means (± standard deviations) obtained on 2−3 independent measurements.

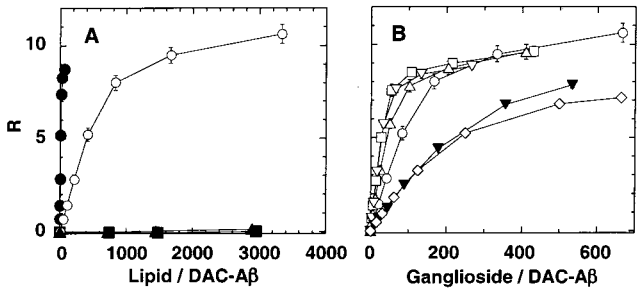

FIGURE 1: Binding of DAC-Aβ to various membranes at 37 °C. DAC-Aβ (0.5 μM) buffer solutions were titrated with GM1 micelles and LUVs of various lipid compositions. Relative fluorescence enhancement, $R = (F - F_0)/F_0$, is plotted as a function of (A) lipid-to-peptide ratio or (B) ganglioside-to-peptide ratio. Fluorescence intensity at 470 nm in the presence and absence of LUVs are denoted by F and F_0, respectively. Lipid composition: closed triangles, SM; closed circles, GM1 micelles; closed squares, GM1/PC (20/80); open circles, GM1/cholesterol/SM (20/40/40); open squares, GD1a/cholesterol/SM (20/40/40); open triangles, GD1b/cholesterol/SM (20/40/40); open inverted triangles, GT1b/cholesterol/SM (20/40/40); closed inverted triangles, GT1b/cholesterol/SM (10/45/45); open diamonds, GM1/GD1a/GD1b/GT1b/cholesterol/SM (5/5/5/5/40/40). Standard deviations for 2−3 preparations are shown by error bars.

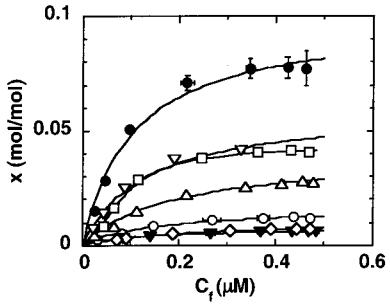

FIGURE 2: Binding isotherms of DAC-Aβ to various ganglioside-containing membranes at 37 °C. Binding isotherms were estimated from the data shown in Figure 1. The bound peptide per exofacial ganglioside, x, is plotted as a function of free peptide concentration, c_f. The traces are the best-fit binding isotherms using eqs 4 and 5 and the parameters shown in Table 1. Symbols are the same as those in Figure 1.

like environment (open circles). In striking contrast, GM1 in PC bilayers did not provide a binding site (squares). SM did not interact with DAC-Aβ (triangles).

Figure 1B shows a comparison of binding of DAC-Aβ to various ganglioside-containing raft-like membranes. Note that the abscissa represents ganglioside-to-lipid ratio. For the systems containing a single ganglioside species at 20 mol %, binding was in the order GM1 < GD1b < GD1a ≈ GT1b. The cholesterol-to-SM molar ratio was always kept constant at 1 to facilitate ganglioside clustering (*11*). Interestingly, a mixture of these four gangliosides at total 20 mol % exhibited the weakest binding (diamonds). A reduction in GT1b content from 20 to 10% also markedly reduced binding (open versus closed inverted triangles).

Binding isotherms were obtained from Figure 1 as follows (*11*). R_{max} values were estimated by linear extrapolation of R versus DAC-Aβ/ganglioside plots (DAC-Aβ/ganglioside → 0) and are summarized in Table 1. The R_{max} values as well as the emission maximal wavelengths (ca. 470 nm) did not differ markedly among the systems, suggesting that the microenvironments of the DAC moiety at the binding sites were similar.

The R/R_{max} ratio gives the bound fraction of the peptide at each data point. Figure 2 shows binding isotherms, i.e., bound DAC-Aβ per exofacial ganglioside (x) versus free DAC-Aβ concentration (c_f) plots. Ganglioside molecules on the outer leaflets (50% of total ganglioside) were assumed to be available for DAC-Aβ binding except for micellar GM1, where all GM1 molecules were available for the peptide. First, the isotherms were analyzed by eq 4 (Langmuir's equation) (*11*, *23*):

$$x = x_{max} Kc_f/(1 + Kc_f) \quad (4)$$

The binding constant and the maximal x value are denoted by K (M^{-1}) and x_{max}, respectively. If the fit was poor (sigmoidal isotherm), the data were reanalyzed by Fowler's equation including the lateral interaction parameter α:

$$\theta = x/x_{max} = [\, K \exp(\alpha\theta)\, c_f]/[\, 1 + K \exp(\alpha\theta)\, c_f] \quad (5)$$

If we put α = 0, eq 5 is reduced to eq 4. The x_{max}, values were estimated by linear extrapolation of x versus $1/c_f$ plots ($1/c_f \rightarrow 0$). The obtained binding parameters are summarized in Table 1.

Detection of Ganglioside Cluster. Excimer formation of BODIPY-GM1 was shown to be useful for detection of the ganglioside cluster (*11*). The excimer (~630 nm)-to-monomer (~520 nm) fluorescence ratio is directly proportional to local dye concentration (*24*). The extents of ganglioside clustering in the two GM1-containing systems were examined by use of BODIPY-GM1, because the x_{max} values of these membranes were different (Table 1). Figure 3 shows the fluorescence emission spectra of BODIPY-GM1-labeled liposomes. The excimer formation in GM1/cholesterol/SM bilayers was promoted to a greater extent than that in the mixed ganglioside system, in keeping with the order of x_{max} value. The anisotropy value of monomer fluorescence, r, as a measure of membrane rigidity was also measured, because excimer formation is facilitated by lower membrane rigidity. The r values of both systems were identical (0.096), indicating that excimer formation solely reflected local BODIPY-GM1 concentration.

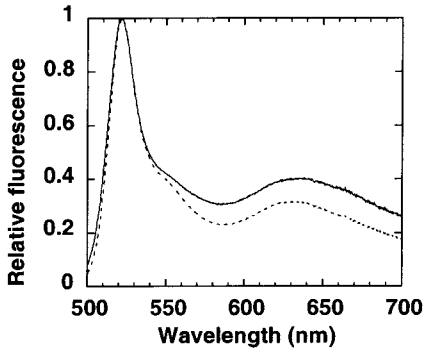

FIGURE 3: Detection of ganglioside clustering. Fluorescence emission spectra of BODIPY-GM1 (1 μM) doped in LUVs were recorded at an excitation wavelength of 480 nm at 37 °C. The spectra were normalized to the monomer peaks (~520 nm). Lipid composition: solid trace, BODIPY-GM1/GM1/cholesterol/SM (5/15/40/40); dotted trace, BODIPY-GM1/GD1a/GD1b/GT1b/cholesterol/SM (5/5/5/5/40/40).

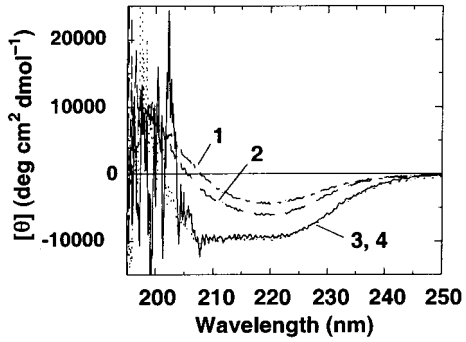

FIGURE 4: CD spectra of native human Aβ-(1−40) in GT1b-containing membranes. CD spectra of the peptides (15 μM) were recorded in the presence of GT1b/cholesterol/SM (20/40/40) SUVs at 37 °C. GT1b/Aβ ratio: trace 1, 5; trace 2, 10; trace 3, 20; trace 4, 40. The spectra are the averages for two preparations, and the errors were within 700 deg cm^2 dmol^{-1} at 220 nm.

Secondary Structure. The conformations of Aβ-(1−40) were estimated from CD spectra. Figure 4 shows data in the presence of GT1b-containing membranes. At lower GT1b/Aβ ratios ($\geq$ 10), the spectra exhibited shallow minima around 218 nm, reminiscent of β-sheets (traces 1 and 2). In contrast, the peptide adopted helical structures at higher GT1b/Aβ ratios ($\geq$ 20), as suggested by double minima around 209 and 222 nm (traces 3 and 4). The absence of an isodichroic point indicated that the helix-to-sheet transition is not a simple two-state process.

Seeding Assay. The seeding abilities of the ganglioside-bound Aβ in raft-like membranes were investigated by ThT assay (Figure 5), which detects aggregated amyloid (*21*). Aβ-(1−40) alone did not show a significant increase in ThT fluorescence during a 1-day incubation, which has been confirmed to be sufficient for seeding assay.[2] The positive control experiment with fAβ as a seed exhibited intense ThT fluorescence. The addition of GM1-containing liposomes under β-sheet-forming conditions (GM1/Aβ = 10) (*11*) also comparably enhanced ThT fluorescence. We confirmed by electron microscopy that these fluorescence enhancements reflected amyloid fibril formation.[2] At a higher GM1-to-Aβ ratio of 80, where a helix-rich structure was induced (*11*), the seeding activity was markedly reduced. Even under β-sheet-forming conditions (ganglioside/Aβ = 5) (Figure 4), the seeding abilities of GD1a- and GT1b-bound forms were much less than that of GM1. A GD1b-bound form showed an intermediate seeding activity.

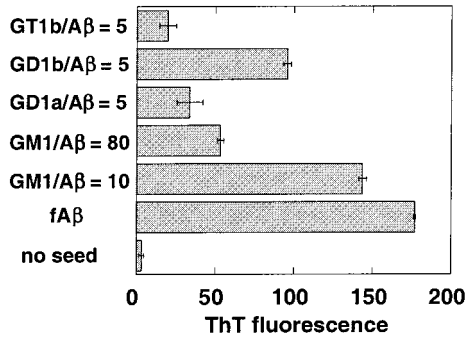

FIGURE 5: Acceleration of Aβ fibril formation in the presence of ganglioside-containing raft-like membranes. Native human Aβ-(1−40) (final concentration, 15 μM) in buffer (10 mM Tris/150 mM NaCl/1 mM EDTA, pH 7.4) was incubated alone or with seeds, i.e., fAβ (0.75 μM) and SUVs composed of ganglioside/cholesterol/SM (20/40/40) at ganglioside/Aβ ratios indicated in the figure for 1 day at 37 °C. Amyloid formation was estimated by ThT fluorescence at 490 nm. The fluorescence intensity of 1 μM calcein solution was set to 1000.

DISCUSSION

We examined the interactions of Aβ with GM1, GD1a, GD1b, and GT1b, the major gangliosides (> 70−80% of total gangliosides) in various parts of the human brain (*25*), in raft-like membranes. The term raft generally refers to the sphingolipid/cholesterol-rich domains believed to exist in cell membranes (*26*). Currently, no method can determine the lipid compositions of rafts, which instead have been inferred from those of detergent-resistant membranes obtained when cell membranes are treated with detergents. For example, the sphingolipid/cholesterol/glycerophospholipid ratio is reported to be 22:58:20 for melanoma MEB-4 cells (*27*) and 17:27:56 for rat cerebellar granule cells (*28*). The ganglioside-to-SM ratio for the latter case is 0.7. However, it should be noted that the detergent-resistant membranes and rafts are not necessary identical, as discussed in detail (*26*). Therefore, our approach using model membranes with various lipid compositions will provide information on the molecular details of Aβ-lipid interactions that plausibly occur in local microdomains of cell membranes, although further tests using neuronal cells are necessary. Our experiments were based on ganglioside/cholesterol/SM (20/40/40) systems because the effects of ganglioside species and cholesterol content can be readily examined around this composition.

Figure 1A clearly shows the importance of a raft-like lipid environment for Aβ-ganglioside interactions. DAC-Aβ effectively bound to the raft-like membrane composed of GM1/cholesterol/SM. Neither SM (Figure 1A) nor cholesterol (*11*) itself constituted a binding site for the protein. In contrast, micellar GM1 interacted strongly with DAC-Aβ (Figure 1A), suggesting that GM1 is absolutely required for DAC-Aβ binding. However, GM1 in PC bilayers did not provide a binding site (Figure 1A). These findings further supported the hypothesis that Aβ recognizes GM1 molecules in a specific physical state, i.e., a cluster (*11*). This idea was also supported by the observations that DAC-Aβ in raft-like membranes showed fluorescence properties (R_{max} and wavelength of maximal fluorescence) very similar to those in GM1 micelles, a large cluster of GM1 (Table 1). We confirmed

that GM1 molecules were not excluded from raft-like membranes to form micelles: DAC-Aβ solution in the presence of raft-like membranes was ultracentrifuged (155000*g*, 30 °C, 1 h), and the fluorescence spectrum of the supernatant was measured. Only the spectrum of free DAC-Aβ (peak at 483 nm) was observed. Comparison of DAC-Aβ binding among various gangliosides revealed the following important aspects. (i) The apparent binding was increased with the number of sialic acid residues (Figure 1B), in keeping with previous data in the PC matrix (*10*, *12*). (ii) The binding affinities were almost constant among the systems investigated (Table 1). Differences in *K* value were only within a factor of 2.2 corresponding to 0.79*RT*. In contrast, the binding affinity of Y10W−Aβ-(1−40) for GM1 doped in PC membranes was reported to be 5−6 times weaker than those for GD1a and GT1b, assuming 1:1 stoichiometry (*12*). (iii) The binding capacities (x_{max}) were highly dependent on lipid composition. For systems containing 20 mol % of a single ganglioside species, the x_{max} value was roughly proportional to the number of sialic acid residues (Table 1). (iv) A decrease in GT1b content from 20 to 10% markedly reduced the x_{max} value, indicating that Aβ recognizes a ganglioside cluster, even if the ganglioside possesses multiple sialic acid residues (Table 1). If individual GT1b molecules constitute binding sites for Aβ, both binding isotherms (Figure 2) would coincide, because the x_{max} value was defined as per the GT1b molecule. (v) Surprisingly, in the mixed ganglioside system, the x_{max} value was much smaller than the expected average of those of individual gangliosides, even smaller than that of GM1 (Table 1). The BODIPY-GM1 experiments (Figure 3) clearly showed that cluster formation was suppressed in the mixed ganglioside system. Thus, lipid composition including cholesterol and gangliosides critically controls Aβ binding. The x_{max} value for micellar GM1 provides an estimate of DAC-Aβ-GM1 binding stoichiometry, because in micelles all GM1 molecules are considered to be involved in a cluster. Table 1 shows that one DAC-Aβ molecule can bind approximately 10 GM1 molecules. One GM1 molecule occupies a cross-sectional area of ca. 75 Å^2 at surface pressures corresponding to lipid bilayers (*29*). Thus, because the protein lies on the membrane (micelle) surface (*10*, *11*), one DAC-Aβ molecule occupies a cross-sectional area of ca. 750 Å^2, i.e., 19 Å^2 per amino acid residue, which is close to the value (20 Å^2) reported for a β-sheet (*30*). The CD spectra indicated that Aβ also undergoes the α-helix-to-β-sheet transition with increases in peptide density on GT1b-containing membranes (Figure 4) as in GM1-containing membranes (*11*). A similar structural transition was reported in phosphatidylglycerol bilayers at low ionic strength (*31*). Therefore, the conformational transition is a general feature of Aβ-membrane interactions. Aβ in GM1-containing raft-like membranes under β-sheet-forming conditions exhibited the strongest seeding activity among the gangliosides investigated (Figure 5), although the Aβ binding ability of GM1 was the weakest (Figure 1B). The fibril formation rate is proportional to free Aβ concentration (*16*). Therefore, the fastest fibril formation in the presence of GM1 is at least partly ascribable to the largest free Aβ concentration. However, differences in free Aβ concentration cannot explain the different fibril formation rates: under the conditions of the ThT assay (Figure 5), free Aβ concentrations were 86 and 30% of total Aβ concentration for GM1/Aβ = 10 and GT1b/Aβ = 5, respectively, as determined by ultracentrifugation (200000*g*, 37 °C, 2 h). The difference in free Aβ concentration was less than 3-fold, whereas the difference in ThT fluorescence was more than 7-fold. The molecular mechanism for this high seeding ability of GM1-Aβ is not clear at present. Slight differences in Aβ conformation that cannot be detected by CD may exist. However, it is pathologically very relevant that GM1-Aβ was discovered in AD and Down's syndrome brains[2] (*4*, *5*).

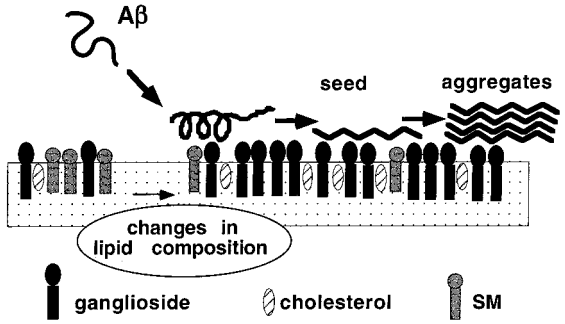

FIGURE 6: A model for ganglioside-mediated amyloid fibril formation. Soluble Aβ with unordered structures does not bind to rafts without ganglioside clusters. Once ganglioside clusters are formed by changes in local lipid composition, such as increases in cholesterol content or ganglioside content, Aβ recognizes the cluster, forming a helix-rich structure. An increase in membrane-bound Aβ density induces a helix-to-sheet conformational transition of Aβ. Under conditions where β-sheet-rich Aβ is observed, especially in the presence of GM1, amyloid fibril formation is markedly accelerated.

We propose a model for membrane-mediated amyloid formation (Figure 6). Soluble Aβ with unordered structures does not bind to rafts lacking ganglioside clusters. Under pathological conditions, changes in local lipid composition, such as increases in contents of cholesterol (*11*), induce ganglioside clusters that Aβ can recognize. The membrane-bound Aβ forms an α-helix-rich structure at lower densities (Figure 3 and ref *11*). At higher densities, Aβ undergoes a conformational transition to the β-sheet-rich structure that can serve as a seed for toxic amyloid fibril formation. It should be noted that this structure determined by CD may contain some contributions from fibrils formed rapidly during CD measurements (ca. 1 h). This model is compatible with the following observations. (i) Lipid rafts rich in gangliosides and cholesterol (*13*) contain soluble (*32*, *33*) and insoluble (*34*) Aβs under physiological and pathological conditions, respectively. (ii) A link between cholesterol, Aβ, and AD has been reported (*35*). (iii) The content of cholesterol in the exofacial leaflets of the synaptic plasma membrane increases during aging, which is a factor facilitating AD (*36*). (iv) Reduction in cholesterol and sialic acid content protects cells from the toxic effects of Aβ (*37*). Our model involving local lipid compositions as a key to amyloid formation may also partly explain selective neuronal degeneration in several human brain regions in AD (*38*−*40*) as well as cell-to-cell differences in susceptibility to Aβ-induced Ca^{2+} influx (*41*). In addition to gangliosides, oxidatively damaged lipids may also facilitate the accumulation of Aβ (*42*). Taking the highest seeding ability of GM1-Aβ (Figure 5) into consideration, GM1-Aβ formation appears to be the key step in the initiation of AD, and its inhibition may be a promising strategy to prevent the development of AD.

REFERENCES

1. Selkoe, D. J. (1994) *Annu. Rev. Cell Biol. 10*, 373−403.
2. Harper, J. D., and Lansbury, P. T., Jr. (1997) *Annu. Rev. Biochem. 66*, 385−407.
3. Lansbury, P. T., Jr. (1997) *Neuron 19*, 1151−1154.
4. Yanagisawa, K., Odaka, A., Suzuki, N., and Ihara, Y. (1995) *Nat. Med. 1*, 1062−1066.
5. Yanagisawa, K., and Ihara, Y. (1998) *Neurobiol. Aging 19*, S65−S67.
6. Yanagisawa, K., McLaurin, J., Michikawa, M., Chakrabartty, A., and Ihara, Y. (1997) *FEBS Lett. 420*, 43−46.
7. McLaurin, J., and Charkrabartty, A. (1996) *J. Biol. Chem. 271*, 26482−26489.
8. ChooSmith, L. P., and Surewicz, W. K. (1997) *FEBS Lett. 402*, 95−98.
9. McLaurin, J., Franklin, T., Fraser, P. E., and Chakrabartty, A. (1998) *J. Biol. Chem. 273*, 4506−4515.
10. Matsuzaki, K., and Horikiri, C. (1999) *Biochemistry 38*, 4137−4142.
11. Kakio, A., Nishimoto, S., Yanagisawa, K., Kozutsumi, Y., and Matsuzaki, K. (2001) *J. Biol. Chem. 276*, 24985−24990.
12. ChooSmith, L.-P., Garzon-Rodriguez, W., Glabe, C. G., and Surewicz, W. K. (1997) *J. Biol. Chem. 272*, 22987−22990.
13. Simons, K., and Ikonen, E. (1997) *Nature* 385, 569−572.
14. Valdes-Gonzales, T., Inagawa, J., and Ido, T. (2001) *Peptides 22*, 1099−1106.
15. Ariga, T., Kobayashi, K., Hasegawa, A., Kiso, M., Ishida, H., and Miyatake, T. (2001) *Arch. Biochem. Biophys. 388*, 225−230.
16. Hasegawa, K., Yamaguchi, I., Omata, S., Gejyo, F., and Naiki, H. (1999) *Biochemistry 38*, 15514−15521.
17. Matsuzaki, K., Murase, O., Tokuda, H., Funakoshi, S., Fujii, N., and Miyajima, K. (1994) *Biochemistry 33*, 3342−3349.
18. Bartlett, G. R. (1959) *J. Biol. Chem. 234*, 466-468.
19. Lakowicz, J. R. (1983) in *Principles of Fluorescence Spectroscopy*; pp 112−155, Plenum Press, New York.
20. Takakuwa, T., Konno, T., and Meguro, H. (1985) *Anal. Sci. 1*, 215−218.
21. LeVine, I. H. (1993) *Protein Sci. 2*, 404−410.
22. Naiki, H., and Gejyo, F. (1999) *Methods Enzymol. 309*, 305−318.
23. Cerny, S. (1983) in *The Chemical Physics of Soild Surfaces and Heterogeneous Catalysis* (King, D. A., and Woodruff, D. P., Eds.) pp 1−57, Elsevier, Amsterdam.
24. Förster, T. (1969) A*ngew. Chem., Int. Ed. Engl. 8*, 333−343.
25. Kracun, I., Rösner, H., Cosovic, C., and Stavjenic, A. (1984) *J. Neurochem. 43*, 979−989.
26. London, E., and Brown, D. A. (2000) *Biochim. Biophys. Acta 1508*, 182−195.
27. Ostermeyer, A. G., Beckrich, B. T., Ivarson, K. A., Grove, K. E., and Brown, D. A. (1999) *J. Biol. Chem. 274*, 34459−34466.
28. Prinetti, A., Chigorno, V., Tettamanti, G., and Sonnino, S. (2000) *J. Biol. Chem. 275*, 11658−11665.
29. Maggio, B., Cumar, F. A., and Caputto, R. (1981) *Biochim. Biophys. Acta 650*, 69−87.
30. DeGrado, W. F., and Lear, J. D. (1985) *J. Am. Chem. Soc. 107*, 7684−7689.
31. Terzi, E., Hölzemann, G., and Seelig, J. (1997) *Biochemistry 36*, 14845−14852.
32. Lee, S.-J., Liyanage, U., Bickel, P. E., Xia, W., Lansbury, P. T., Jr., and Kosik, K. S. (1998) *Nat. Med. 4*, 730−734.
33. Morishima-Kawashima, M., and Ihara, Y. (1998) *Biochemistry 37*, 15247−15235.
34. Sawamura, N., Morishima-Kawashima, M., Waki, H., Kobayashi, K., Kuramochi, T., Frosch, M. P., Ding, K., Ito, M., Kim, T. W., Tanzi, R. E., Oyama, F., Tabira, T., Ando, S., and Ihara, Y. (2000)- *J. Biol. Chem. 275*, 27901−27908.
35. Wolozin, B. (2001) *Proc. Natl. Acad. Sci., U.S.A. 98*, 5371−5373.
36. Igbavboa, U., Avdulov, N. A., Schroeder, F., and Wood, W. G. (1996) *J. Neurochem. 66*, 1717−1725.
37. . Wang, S. S.-S., Rymer, D. L., and Good, T. A. (2001) *J. Biol. Chem. 276*, 42027−42033.
38. Ball, M. J. (1977) *Acta Neuropath. 37*, 111−118.
39. Price, D. L., Whitehouse, P. J., Struble, R. G., Clark, A. W., Coyle, J. T., DeLong, M. R., and Hedreen, J. C. (1982) *Neurosci. Commun. 1*, 84−92.
40. Arendt, T., Bigl, V., and Tennstedt, A. (1983) *Acta Neuropath. 61*, 101−108.
41. Kawahara, M., Kuroda, Y., Arispe, N., and Rojas, E. (2000) *J. Biol. Chem. 275*, 14077−14083.
42. Koppaka, V., and Axelsen, P. H. (2000) *Biochemistry 39*, 10011−10016.

BI0255874